7.6 AEROSOL IMPACTS ON TROPICAL CYCLONES

William R. Cotton, Gustavo G. Carrió, and S Herbener
Department of Atmospheric Science, Colorado State University, Fort Collins, Colorado

1. INTRODUCTION

Previous simulations by Zhang et al (2007; 2009) revealed a non-monotonic response to dust acting as CCN inserted into a hurricane environment. We hypothesize that much of that variability was due to the variable intensity of outer rainband convection when the enhanced CCN advected into that region. Earlier modeling studies of deep convection suggests that CCN can both enhance and weaken convection depending on the intensity of convection, with weak convection being weakened by enhanced CCN and more vigorous convection intensified. Virtually none of the dust made its way into the interior of the storm owing to strong washout.

Motivated by Zhang et al's simulations, Cotton et al., 2007) hypothesized that seeding hurricanes with pollution-sized aerosols could lead to the following responses:

- In the outer rainbands, increasing CCN concentration results in reduced collision/coalescence, increased supercooled water aloft, enhanced convection (latent heat of freezing) and ultimately enhanced precipitation and low level cooling (evaporation).
- The increase in low level cold-pool coverage in the outer rainband region blocks the flow of energy into the storm core inhibiting the intensification of the TC.
- However, the amount of suppression of the strength of the TC depends on the timing between the transport of CCN to the outer rainbands and the intensity and lifecycle stage of the outer rainband convection.
- The outer rainband convection needs to be strong in order for the transport of supercooled liquid water aloft to take place.

* *Corresponding author address:* William R. Cotton, Department of Atmospheric Science, Colorado State University, Fort Collins, CO 80526; email: cotton@atmos.colostate.edu.

In this paper and in the accompanying talk we simulate targeted seeding of outer rainband convection to help us better understand the response of hurricanes to CCN seeding. As a result we designed a series of simulations for which the time of the "virtual flights" as well as the aerosol release rates are varied. RAMS@CSU was configured to have three two-way interactive nested grids. All runs consider a spin-up time of 36 hours and after that time, seeding is considered. A code that simulates the flight of a plane is used to increase the CCN concentrations as an aircraft flies. We performed various runs considering virtual flights at an altitude slightly lower than cloud base and at several seeding times (every three hours). In addition, the aerosol release rates were also varied. All sensitivity experiments considered an aircraft speed of 150m/s and flight times ranging from 10 to 30 min, increasing as the tropical cyclone develops.

Results show a significant sensitivity to both the seeding time and the aerosol release rates. Supporting the aforementioned hypotheses, seeding flights increased the quantities of supercooled liquid water, peak updrafts, and lowered the temperature of the cold pool and, more importantly, the peak surface winds.

2. METHODS

2.1 *Mesoscale Model*

The Regional Atmospheric Modeling System developed at Colorado State University (RAMS@CSU, Pielke et al., 1992; Cotton et al., 2003) was used to examine the chain of responses to the introduction of enhanced CCN concentrations in TCs. The idealized tropical storm simulations were similar to those of Zhang et al (2007; 2009) except for recent updates in the model. Three nested grids were employed, the horizontal grid spacings were 24, 6 and 1.5 km for grids 1 to 3, respectively. The corresponding time

steps were 60, 20, and 5s. The storm and the finest grid centers were approximately coincident (~ 15N, 40W).

The simulation period covered 72h, but the first 36h were considered a spin-up time. All the microphysical species (cloud water, rain, pristine ice, snow, aggregates, graupel and hail) in RAMS@CSU were activated, and both hydrometeor mixing ratios and number concentrations were predicted through the use of the two-moment bin-emulating bulk microphysics scheme (Saleeby and Cotton, 2004, 2008). CCN, GCCN and IFN concentrations are all considered prognostic variables in RAMS@CSU.

For this study we implemented a prognostic scheme (based on the O' Dowd diagnostic formulae) to take into account sea-spray sources for the film, jet, and spume modes which at as CCN and GCCN, respectively. In addition, we added modules to take into account the scavenging of various types of aerosols by drizzle and raindrops. These routines (separately) compute scavenging of CCN, GCCN as well as the film, jet, and spume sea-spray modes by drizzle and raindrops spectra. Scavenging coefficients are calculated as functions of aerosol size and precipitation rates at each model grid cell; they use curves derived from empirical data (Chate, personal communication).

2.2 *Experimental Design*

All numerical experiments were homogeneously initialized with clean (maritime) concentrations. A code that simulates the flight of a plane was used to increase the CCN concentrations as an aircraft flies following different trajectories at various seeding times. In addition, the aerosol release rates were also varied. The virtual flights were performed at an altitude slightly lower than cloud base height. All sensitivity experiments considered an aircraft speed of 150m/s and flight times ranging from 10 to 30 min, increasing as the tropical cyclone develops. Figure 1 schematically represents two internal radius and external virtual flights. Runs varied the seeding time and some runs combined internal and external flights.

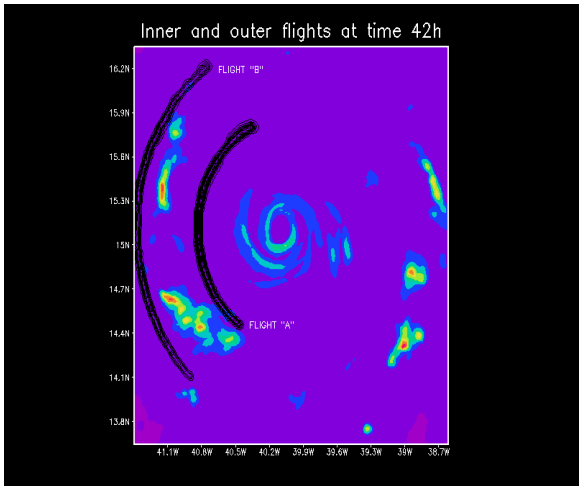

Figure1: Virtual flights 42a and 42b. For the combined trajectory, the aircraft would fly north following flight "A" and then south along flight "B". Black contours denote aircraft flight paths and shaded areas locate convective activity at that time (LPWs).

3. RESULTS

3.1 Updrafts and precipitation

All runs considering virtual flights indicated that seeding increases both the magnitude of the updraft maxima and the altitude at which they occur. This enhancement was associated with an important increase in the supercooled liquid water contents (not shown). Earlier virtual flights tend to be more efficient. More importantly, the impact of seeding on the maximum simulated precipitation (whose reduction can be considered as an indicator of storm intensity mitigation) was significant. This reduction was sensitive to both the time at which the flight was performed and the trajectory covered by aircraft. It was most important for outer trajectory at time 39h. As an example, Figure 2 compares the temporal evolution of the integral value of the precipitated mass produced by numerical experiment considering external trajectories at time 39h for various aerosol release rates. In all cases, the integral mass of precipitation decreased by

seeding, although it did not show a regular response to different [CCN].

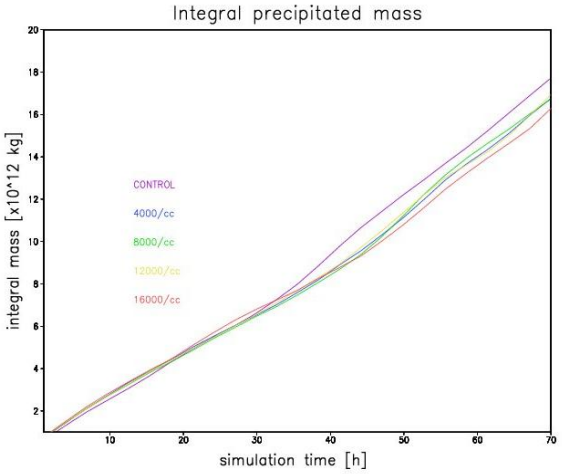

Figure 2: Temporal evolution of the integral precipitated mass of water.

3.2 Cold-pools

We generated and compared probability density functions (PDFs) of cold-pool size for 10 runs using grid 3 model outputs. The main results can be summarized a follows:

● All simulated seeding flights produced cold-pool distributions with expected (mean) values considerably higher (warmer) than that of the control run (no seeding). The only exception was exp 10. For one flight at 39h (8000/cc), the expected area is four times larger than that of the control run (exp 1).

● The PDFs of cold-pool area also showed differences in their tails, indicating higher frequencies of large cold-pools sizes (not shown). The maximum area behaved in a similar manner with considerable increases for all sensitivity runs except for the run with an aerosol release rate 50% lower (exp#10). The latter fact suggests a lower limit for seeding intensity.

● Not only is the cold pool-size affected by seeding but so also its minimum temperature. We computed those minima, relative to the current domain (grid 3) horizontal average. In most cases (again, exp #10 is an exception) this difference (ΔT_{pool}) was higher (in absolute value) than that corresponding to the control run.

● Virtual seeding flights reduced the temperature of the entire lower layer. The horizontally-averaged temperature over the finest grid for the first model level above ground relative those of the control run for the last 24h of the simulation (ΔT_{G3}) gave negative differences for all runs (including exp#10). These differences (up to 0.14ºC) may seem small, however, it must be noted that they are domain averages. These differences appear be the cause of the storm intensity weakening. Moreover, the seeding effects on expected and maximum cold-pool areas are actually underestimates because the have been computed relative to each run's horizontal average.

These results are summarized in Table I, for different seeding times, trajectory types, and aerosol release rates.

Table I: Cold pools analyses for flights varying aerosol release rates

Exp	Time	Type	[#/cc]	Expected area[km^2]	Maximum area[km^2]	ΔT_{pool} [ºC]	ΔT_{G3} [ºC]
1	-	-	0	26.3	49.5	-5.29	0.00
2	36	int	8000	50.6	288.0	-5.68	-0.06
3	36	ext	8000	67.1	180.0	-5.45	-0.05
4	42	ext	8000	76.1	292.5	-6.77	-0.03
5	39	both	8000	49.8	141.8	-5.38	-0.06
6	36	both	8000	26.8	67.5	-5.29	-0.03
7	42	both	8000	100.4	357.7	-5.57	-0.02
8	39	ext	8000	69.5	357.8	-5.68	-0.14
9	39	ext	6000	88.9	299.3	-5.66	-0.13
10	39	ext	4000	25.9	49.5	-5.10	-0.05

The row highlighted in blue corresponds to the flight that generated the strongest impact (external flight at 39h, 8000/cc). We performed several other experiments using this virtual flight but varying the CCN concentration along the trajectory between 2000 and 16000/cc. The results are summarized in Table II. It is interesting to note the clearly monotonic behavior of the various quantities compared in Table II when CCN concentrations vary between 2000 and 8000/cc. However, it can be seen that there is a change of response above 8000/cc. In particular, the area of the largest cold-pool simulated for the 8000/cc run is six times higher than that of the control run. However, it decreases approximately 10% from 8000 and 12000/cc. The overall cooling (ΔT_{G3}) for 8000/cc doubles that of the 2000/cc run.

Table II: Cold pools analyses for flights varying aerosol release rates

[#/cc]	Mean area [km^2]	Max area [km^2]	ΔT_{pool} [ºC]	ΔT_{G3} [ºC]
0	26.3	49.5	-5.29	0.00
2000	26.2	49.5	-5.19	-0.05
4000	25.9	69.5	-5.32	-0.05
6000	88.9	299.3	-5.66	-0.13
8000	69.5	**357.8**	**-5.68**	**-0.14**
10000	72.3	352.4	-5.72	-0.12
12000	68.0	333.2	-5.68	-0.12

3.3 Downdrafts

We compared overall downward fluxes to examine the monotonic behavior for concentrations less than 8000/cc (along the flight trajectory) and the suggested opposite response behavior above this threshold. Figure 3 gives the time-averaged vertical profiles of the downward mass flux for runs considering concentrations up to 8000/cc.

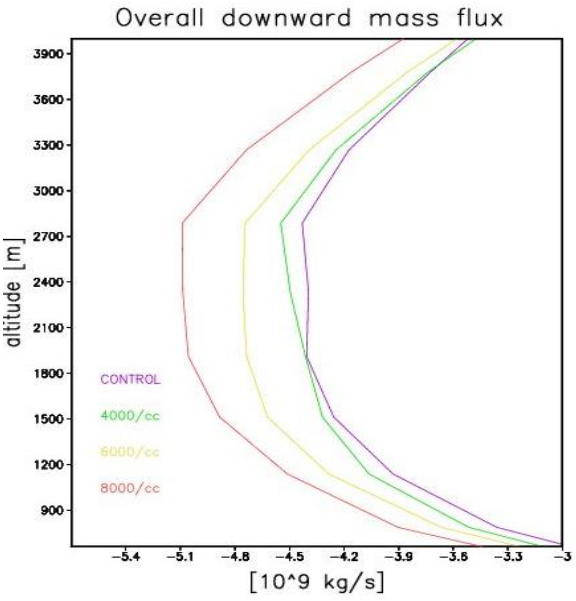

Figure 3: Time-averaged mass fluxes.

Larger downward fluxes were simulated when virtual lights used higher CCN release rates (differences up 15% compared the control run). The response is clearly monotonic, except for very large release rates where the behavior changes.

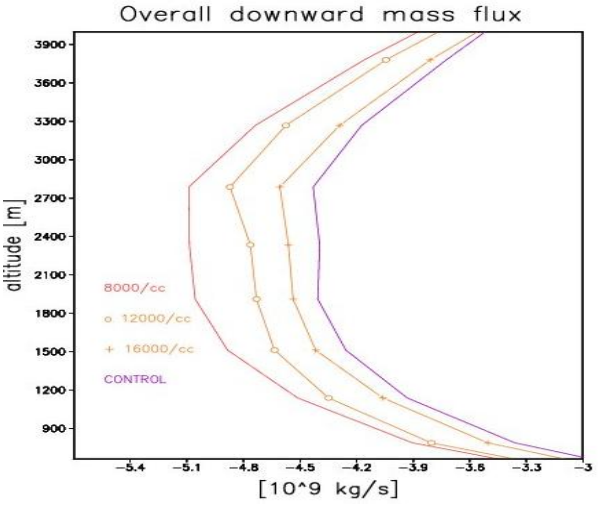

Figure 4: Idem Fig 3 but for [CCN] above 8000/cc.

Figs 5 and 6 show that the enhanced downward fluxes are not linked (only) to more intense downdrafts but also to larger areas covered by them. The response is again clearly monotonic up to 8000/cc. All virtual flights produced larger downdraft coverage. However, for [CCN] along the trajectory above 8000/cc, it decreases.

We generated statistics selecting the downdrafts linked to cold-pools of larger area at each model output time (grid3). As an example, Figure 7 shows the downdraft associated to the largest simulated cold-pool (seeding at 39h, 8000/cc). Figure 8 is a detail of the first 4 km and shows this cold pool.

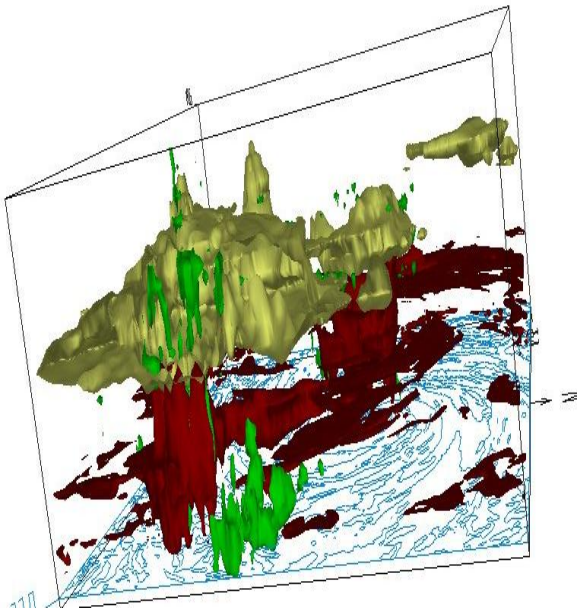

Figure 5: Updrafts (red), downdrafts (green), and pristine ice (yellow) at simulation time 60h. Isosurfaces correspond to -2m/s, 3m/s, and 0.2g/kg for downdrafts, updrafts, and pristine ice mixing ratio, respectively.

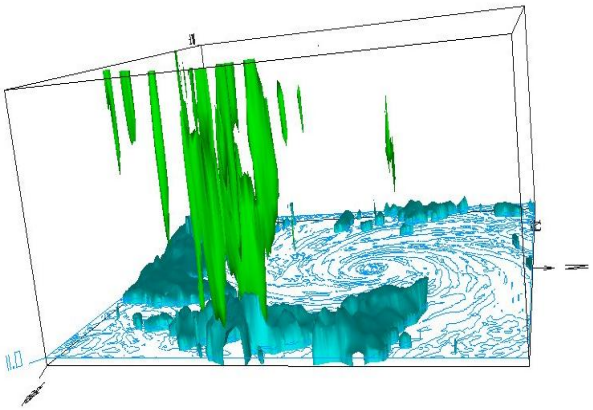

Figure 6: Downdrafts (green) and cold pools (light blue) for the same time and run of Fig. 5. Isosurfaces correspond to -2m/s, and -5ºC for downdrafts and cold pool temperature difference (with respect to the horizontal average), respectively.

Figures 7 and 8 compare time-averaged buoyancy vertical profiles for runs with [CCN] above and below 8000/cc, respectively.

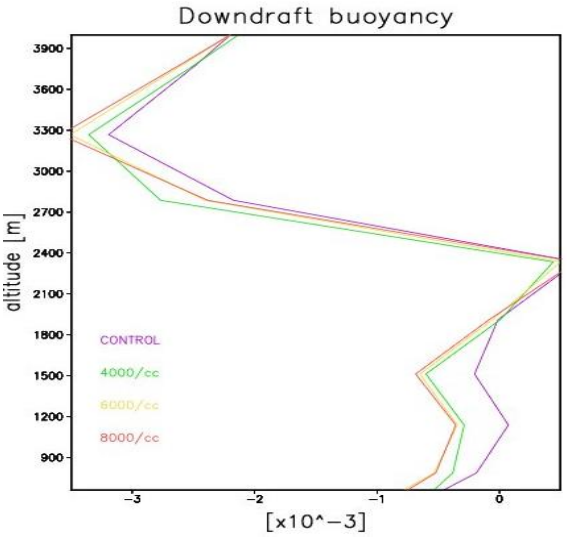

Figure7: Vertical profiles of buoyancy (non dimensional) within downdrafts for numerical experiments considering different aerosol release rates.

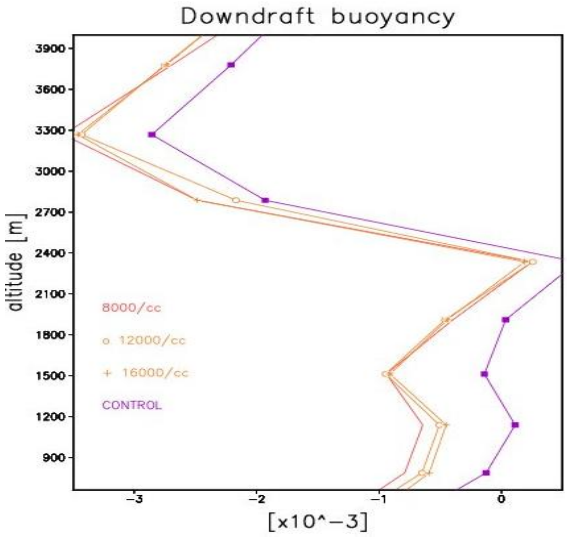

Figure 8: Idem Fig. 7 but for runs with [CCN] above 8000/cc.

Higher (more negative) values of buoyancy were simulated for runs with [CCN] along the flight trajectory lower or equal to 8000/cc. All sensitivity runs produced higher values of buoyancy, however, further enhancing aerosol concentrations produces the opposite effect.
Figures 9 and 10 are analogous to Figs, 7 and 8 but they give rain mixing ratio vertical profiles.

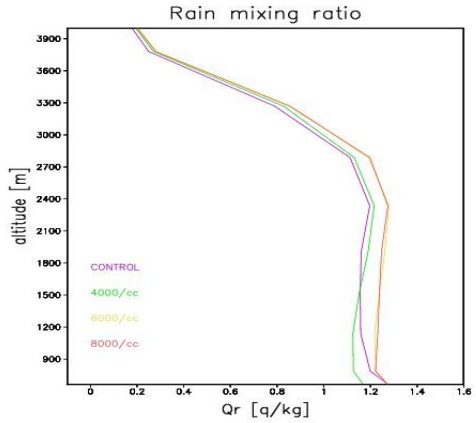

Figure 9: Vertical profiles of rain mixing ratio within downdrafts for numerical experiments considering different aerosol release rates.

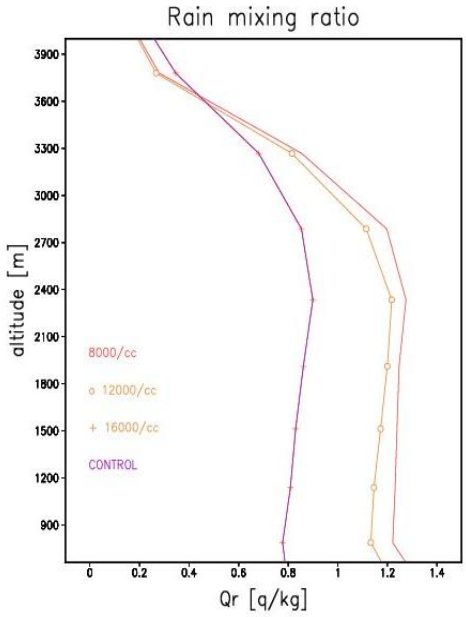

Figure 10: Idem Fig. 9 but for runs with [CCN] above 8000/cc.

It can be seen that rain mixing ratios exhibit an identical pattern of response.

3.4 Surface winds

We computed and compared PDFs for surface winds. All numerical experiments produced a reduction in the frequencies of hurricane-intensity surface winds. Figure 11 compares surface wind frequencies corresponding to seeding flights to those of the control run.. A minimum reduction 20% was simulated for all hurricane categories. Figure 12 compares the surface wind distributions obtained for the control run and 4 virtual flights with [CCN] below 8000/cc. The frequencies of the highest surface winds for the control run are approximately 6 times larger than those corresponding to the 8000/cc run. Figure 13 is analogous to Fig 12 but for the higher [CCN] range. Again, an opposite response can be observed for then 12000 and 16000/cc run.

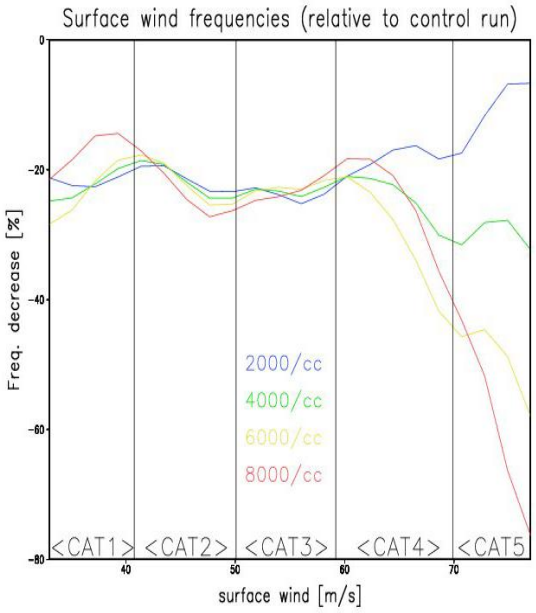

Figure 11: Percent decrease in the wind surface frequencies with respect to the control run.

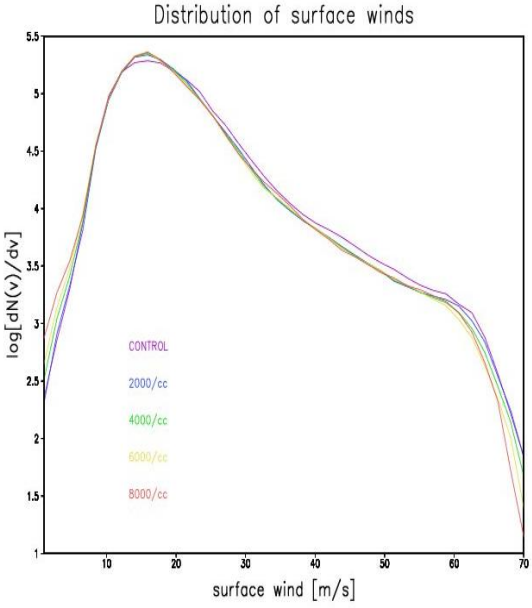

Figure 12: Surface wind distributions for runs with [CCN] up to 8000/cc.

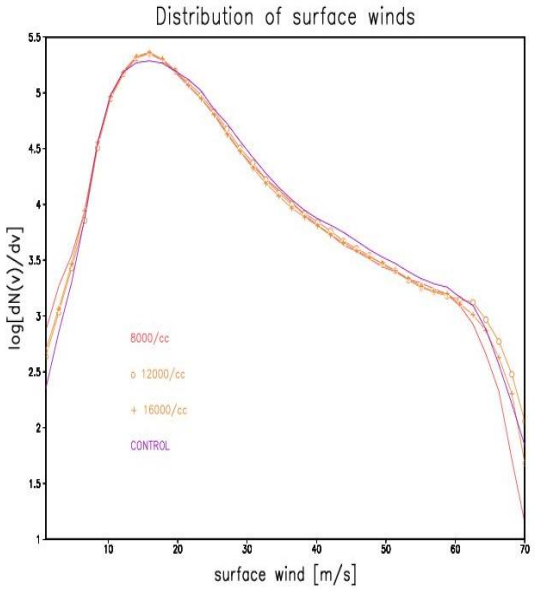

Figure 13: Idem Fig 12 but for runs with [CCN] above 8000/cc.

4. CONCLUSIONS

The results of this study support the hypothesis described in Section 1.. Virtual flights cause a reduction of collision and coalescence, resulting in more supercooled liquid water to be transported aloft. This supercooled liquid water enhances latent heat of freezing producing higher updraft maxima that occur at higher altitudes. Results also suggest that the higher evaporative cooling from the increased precipitation in the outer rainbands produces stronger and more widespread cold-pools. These cold-pools, covering larger areas, block the flow of energy into the storm core and therefore inhibit the intensification of the storm.

The change of behavior for runs with [CCN] above 8000/cc appears to be linked to the mechanism suggested by Carrió et al (2010) and Carrió and Cotton (2010). Further enhancing CCN concentrations reduce riming growth of ice particles to the extent that this process would became inefficient. Therefore, a greater fraction of the ice-phase water mass is transported upwards to anvil levels as pristine ice crystals instead of being precipitating to the surface. In addition, the enhancement in the concentration of (smaller) pristine ice crystals transported to higher levels of

the storm may lead to an increase in optical thickness, area coverage, and life time of the cirrus-anvil clouds (as suggested by Carrió et al., 2007).

In summary, the primary impact of aerosols on TC genesis and intensity is by altering the strength of cold-pools! The idea that cold-pools are an important modulator of TC intensity is consistent with observations that TC genesis occurs follows the formation of a nearly saturated core(results in weak cold-pools). It is also consistent with strong vertical wind shear as being a detriment to TCs(strong shear enhances entrainment of dry air increasing cold-pool strengths).

During TC genesis vigorous cold-pools can lead to vertical decoupling between a mid-level MCV and low-level vorticities. Vigorous cold-pools in mature TCs can lead to blocking of moist low-level flow into the storm interior and/or causing a decoupling between a surface-based vortex and the cyclone aloft

An implication from this research is that greater attention has to be taken in cold-pool diagnosis for hurricane strength prediction. A remote sensing method of TC cold-pools would be ideal to map cold-pool variability in TCs Furthermore, in order to simulate and predict aerosol impacts on TCs, models need high enough resolution and microphysics to represent convective-scale dynamical responses to aerosols as well as environmental properties affecting cold-pools

5. ACKNOWLEDGEMENTS

This work was supported by a grant funded by the Department of Homeland Security through NOAA (NOAA-ESRL) contract # NA17RJ1228.

6. REFERENCES

Carrió, G. G., Cotton, W. R., Cheng W. Y. Y., 2010: Urban growth and aerosol effects on convection over Houston. Part I: the August 2000 case. Atmos. Res., 96, 560-574.

Carrió, Cotton, W. R., 2010: Effects of the Urban growth of Houston on convection and precipitation. Part II: Their dependence on instability. Submitted to Atmospheric Research.

Carrió, G.G., S.C. van den Heever, and W.R. Cotton, 2007: Impacts of nucleating aerosol on anvil-cirrus clouds: A modeling study, *Atmos. Res.*, **84**, 111-131.

Cotton, W.R., H. Zhang, G.M. McFarquhar, and S.M. Saleeby, 2007: Should we consider polluting hurricanes to reduce their intensity? *J. Wea. Mod*., **39**, 70-73.

Cotton, W.R. and R.A. Pielke, 2009: Human impacts on weather and climate, Cambridge University Press, New York, 288 pp.

Cotton, W.R., R.A. Pielke Sr., R.L. Walko, G.E. Liston, C.J. Tremback, H. Jiang, R.L. McAnelly, J.Y. Harrington, M.E. Nicholls, G.G. Carrió, and J.P. McFadden, 2003: RAMS 2001: Current status and future directions. *Meteor.. Atmos. Phys*., **82**, 5-29.

Meyers, M. P. Walko, R. L., Harrington J. Y. , Cotton, W.R., 1997: New Rams cloud microphyisics parameterization : Part II. The two-moment scheme. *Atmos. Res.*, **45**, 3-39.

Pielke, R. A., Cotton, W. R., Walko, R.L., Tremback, C. J. Lyons, W.A. Grasso, L. D. Nicholls, M. E., Moran, M.D., Wesley, D. A. , Lee, T.J., Copeland, J. H.,1992: A comprehensive meteorological modeling system-RAMS. *Meteorol. Atmos. Phys.*, **49**, 69-91.

Saleeby, S. M., and W.R. Cotton, 2008: A Binned Approach to Cloud-Droplet Riming Implemented in a Bulk Microphysics Model. *J. Appl. Meteo,* **47**, 694-703.

Saleeby, S. M., and W.R. Cotton, 2004: A large-droplet model and prognostic number concentration of cloud droplets in the RAMS@CSU model. Part I: Module descriptions and Supercell test simulations. *J. Appl. Meteo,* **43**, 182-195.

Zhang H., G. M. McFarquhar, S. M. Saleeby, W. R. Cotton, 2007: Impacts of Saharan dust as CCN on the evolution of an idealized tropical cyclone. *Geophys. Res. Lett*., **34**, L14812, doi:10.1029/2007GL029876.

Zhang, H., G. M. McFarquhar, W. R. Cotton, and Y. Deng (2009), Direct and indirect impacts of Saharan dust acting as cloud condensation nuclei on tropical cyclone eyewall development, Geophys. Res. Lett., 36, L06802, doi:10.1029/2009GL037276